Arabian Journal of Geosciences (2022) 15:1109
https://doi.org/10.1007/s12517-022-10400-2

ORIGINAL PAPER

Characterization of iron-modified natural clay for textile dye retention by sono-adsorption technology

Mabrouk Eloussaief[1] · Wiem Hamza[1] · Nadim Fakhfakh[1] · Ali Tlili[2] · Nejib Kallel[2] · Stephanie Lambert[3] · Hicham Zaitan[4] · Mourad Benzina[1]

Received: 13 November 2021 / Accepted: 19 May 2022

Abstract

In the present study, iron-pillared clay was prepared using ferrous nitrate $Fe(NO_3)_3$. The removal of Reactive Blue (RB4) dye by ultrasound-assisted sorption onto the synthesized pillared Tunisian clay in aqueous solutions was studied. The natural and modified clay samples were characterized using XRD, FTIR TEM, and nitrogen adsorption measurement methods. Mineralogical data show that smectites are the main minerals of clay samples. FTIR spectra indicate that the stretching vibration bands of the structural hydroxyl groups are broad after treatments. A new band appears at 1570 cm^{-1}, after the sorption of RB4 dye, attributed to aromatic C = C stretching vibration, which suggests the adsorption of RB4. A remarkable decrease was detected in the BET surface after sono-adsorption indicating that the sites of modified clay are almost occupied by the dye. The maximum Reactive Blue 4 quantity was removed at pH 8. Meanwhile, more active Fe–C surface sites were available for both adsorption and sono-adsorption with increasing RB4 concentration, thereby increasing the removal efficiency. Monolayer adsorption capacity via the sono-assisted method also showed a high removal amount of 46.51 mg/g. Langmuir's model describes the experimental data better than Freundlich's. A comparative study confirmed that RB4 sono-adsorption by a Tunisian clay sample was higher than others used in other relevant studies, highlighting that these clay deposits may be applied to the dyes' elimination from wastewaters.

Keywords Clay · Adsorption · Sono-assisted adsorption · Reactive Blue

Introduction

Releasing colored wastewater inside water resources has, consequently, detrimental effects on the environment, toxicity to flora, and prospective risk to human health. Different treatment techniques were used for dye elimination, such as ozonation, biological processes, and adsorption by using different adsorbents like clay, and activated carbon (Roosta et al. 2014; Eloussaief et al. 2018). Ultrasound irradiation is a process that can be combined with natural clays to improve the effectiveness and extend the applicability of these materials. This can be used due to the synergetic effect of both ultrasound and clays (Asfaram et al. 2015; Chatel et al. 2016; Chu et al. 2017). Sono-chemistry improves mass transfer through shock waves with significant improvements in the material properties (Soltani et al. 2016; Jorfi et al. 2017).

In this context, ultrasound-assisted adsorption by using natural clay has been extensively studied (Ali et al. 2014, Chatel et al. 2016). Improvement of particle reduction is associated with several other physical modifications like

Responsible Editor: Amjad Kallel

✉ Mabrouk Eloussaief
eloussaiefmabrouk@yahoo.fr

[1] Laboratoire de Recherche Eau, Energie et Environnement, LR99ES35, Ecole Nationale d'Ingénieurs de Sfax, Université de Sfax, BP W, Sfax 3038, Tunisie

[2] Laboratoire de Recherche GéoressourcesMatériauxEnvironnements Et Changements Globaux, LR13ES23, Faculté Des Sciences de Sfax, Université de Sfax, Sfax BP11713000, Tunisie

[3] Laboratory of Chemical Engineering, Catalytic Engineering Institute of Chemistry, University of Liege, Liege, Belgium

[4] Processes, Materials and Environment Laboratory (LPME), Department of Chemistry, Faculty of Sciences and Technology of Fez, Sidi Mohamed Ben Abdellah University, Fez, Morocco

Published online: 03 June 2022

dispersion and particle reduction. Eren 2012 conducted an extensive review on the potential application of ultrasound technique for the dyes' removal in aqueous systems. Power ultrasound (20–100 kHz) is a handy tool to bring about some chemical and physical changes due to its ability to generate cavitations of bubbles (Wu et al. 2013). Thus, the sono-chemical treatment may pave the way for new applications of natural clays. Among these new routes, one can refer to the dyes' elimination in aqueous conditions (Almazán-Sánchez et al. 2016; Bethi et al. 2018), the presence in aquatic environments may cause deleterious environmental problems. Adsorption and sono-adsorption are being applied as technologies of choice for organic compound removal from industrial wastewaters (Sajjadi et al. 2017; Dil et al. 2018; Eloussaief et al. 2020b).

Furthermore, low cost and naturally abundant clay deposits were extensively applied to sewage treatment owing to advantageous surface characteristics (Machado et al. 2011; Dietel et al. 2017). Similarly, several natural clay deposits, in Tunisia, were excavated for their potential application as dyes adsorbents (Adeogun et al. 2020), VOC (Jarraya et al. 2016), heavy metals (Kashif Uddin 2016), and many other applications (Loungou et al. 2017; Eloussaief et al. 2020a). However, no attempt has been made to evaluate the efficiency of those natural clays via a sono-chemical treatment of organic dyes (sono-adsorption).

Surface modification of clays with certain polyhydroxy cations can be useful for improving the adsorptive efficiency (Hamza et al. 2016). The iron pillaring process has led to an augmented adsorptive efficiency (Almazán-Sánchez et al. 2016).

Modified clays proved their favorable application as fillers of organic compounds. Thus, it received special attention, mainly for the dye removal. To the best of our knowledge, the application of ultrasound-assisted adsorption of RB4 by Tunisian natural clay has never been investigated. Thus, we propose to study the potential use of modified clay from the Cherahil area (central Tunisia) in the removal of RB4 under silent and ultrasound-adsorption. The effects of the main influential adsorption parameters, including pH, adsorbent amount, and initial dye concentration were evaluated in batch sorption methodology for silent adsorption and clay-ultrasound combined experiments. Theoretical kinetic models and equilibrium isotherms were successfully applied for the experimental data.

Materials and methods

Geology description of Cherahil area

In the Cherahil location (central Tunisia), the El Haria formation conformably overlaid the chalky white limestone of the Abiod formation (Amami-Hamdi et al. 2016). The overlaying Paleocene clayey to marly series exceeding 50 m-thick section forms the main body of the El Haria clays (Fig. 1). These deposits preceded the Eocene phosphatic limestone (i.e., Metlaoui formation).

Materials

The natural material clay used in this investigation was collected from the Cherahil region. Acetic acid, sodium hydroxide (NaOH), ferrous nitrate $Fe(NO_3)_3$ (C98%), and RB4 dye were all supplied by the society Sigma-Aldrich, Tunisia. The RB4 chemical structure is shown in Fig. 2.

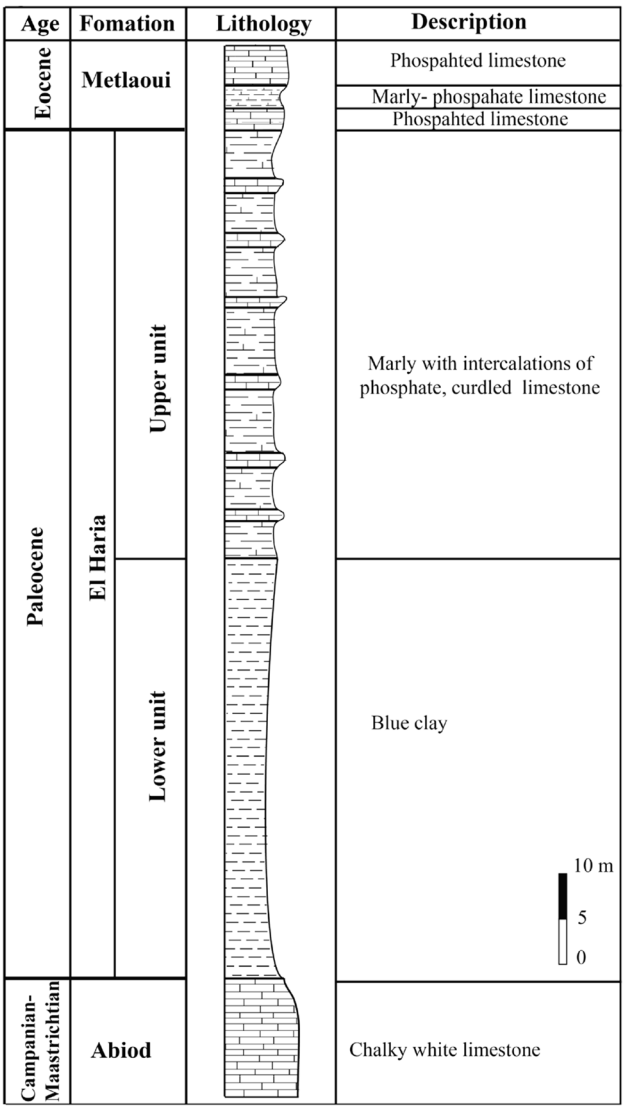

Fig. 1 Cross section of studied sample

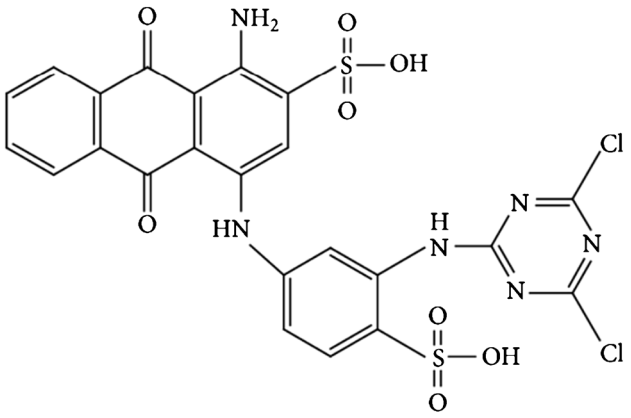

Fig. 2 Reactive Blue 4 chemical structure

Preparation of adsorbent and synthetic effluent

The collected original clay sample followed a routine treatment to extract the desired less than 2 µm-sized clay fraction. Chemically, the studied "Cherahil clay" consists of 45.4% SiO_2; 16.72% Al_2O_3; 4.7% Fe_2O_3; 4.8% CaO; 4.50% MgO; 2.8% Na_2O; 1.2% K_2O, and 18.42% loss of ignition.

Reactive Blue 4 dye with molecular formula of $C_{23}H_{14}Cl_2N_6O_8S_2$ and molecular weight of 637.43 g/mol is a commercial anthraquinone dye from Sigma-Aldrich, Malaysia. The aqueous dye solutions (200 mg/L) were prepared in double deionized water.

Preparation of iron-clay

The Fe–C solution consists of the addition of 0.74 mol/L sodium hydroxide (NaOH) solution into 0.4 mol/L ferric nitrate ($Fe(NO_3)_3$) solution. The reaction process was maintained under stirring even as the NaCl solution was pumped, providing [OH^-]:[Fe(III)] 2:1.

The suspension of raw clay was heated to 50 °C and the pillared solution was added under strapping stirring 1.0 mL/min to provide a 10 mmol of iron/g of used clay. The prepared solution rested for 6 days at 25 °C (Ullhyan, 2014; Hamza et al. 2016).

The prepared suspensions of clay-intercalating solution were centrifuged for 16 min at 1000 r/min, the solid phase was washed 5 times with ultra pure water. The prepared iron modified clay was firstly crushed, dried for 24 h at 100 °C, fired at 350 °C for 4 h, and finally stored. The iron modified clay prepared with [OH-]:[Fe(III)] 2:1 was named Fe–C or modified clay.

Characterization of adsorbent

The used clay was characterized by using different methods such as X-ray Fluorescence (XRF, ARL® 9800 XP spectrometer). The mineralogical composition and the changes of interlayer spacing in the raw material were investigated using a Rigakud-Max® 2200 model X-ray diffractometer. X-ray diffractograms were obtained on oriented samples.

The study of clay structure is determined by using HRTEM, JEOL JEM 2011. Nitrogen adsorption on a micrometrics ASAP 2020 helped to determine the specific surface area. The surface functional groups were studied using Fourier Transforms Infrared (FT-IR) spectroscopy (Agilent Technologies Cary 630, FT-IR spectrometer).

Sono-adsorption process

The RB4 adsorption onto used modified clay was realized by using a batch technique to assess its reliability. The sono-adsorption experiments were carried out by using the ultrasonic process with a nominal power of 230 W (ULTRASONIC CLEANER USC-T, USC300T) and an output frequency of 45 kHz. The dimensions of the bath are $15 \times 15 \times 15$ cm^3.

A magnetic stirrer (FALC stirrer, 20 W, 50/60 Hz) with 300 rpm was used to evaluate the current adsorption method. All experiments of sono-adsorption were executed in 150 mL container flasks by blinding a variety amount of the adsorbent with 105 mL of RB4 solution. Samples of 5 mL were collected every 5 min and then the adsorbent was removed from the solution of RB4 by percolation.

The determination of the residual dye concentration was carried out by using a Shimadzu 160A UV/visible spectrophotometer such as λ_{max} of RB 4 = 599 nm (Becelic-Tomin et al. 2014; Ben Ameur et al. 2017). Equation (1) was indented to acquire the amount removal of RB4 and the dye adsorbed per unit mass of the adsorbent (mg/g) at equilibrium (1):

$$\text{Capacity of adsorption } (mg/g) = q_e = \left(C_o - C_e\right) \times \frac{V}{m} \quad (1)$$

where C_0 (mg/L), C_t (mg/L), and C_e (mg/L) are the concentrations of the RB4 dye initially, at a time t and at equilibrium, respectively, q_e is adsorption capacity (mg/g), V is the volume of the RB4 solution (L), and m is the mass of adsorbent (g).

Results and discussion

Physicochemical characterization

The crystalline structure of the natural Tunisian clay characterized by XRD (Fig. 3) confirmed that the used raw clay consists of smectite, kaolinite, and illite. The smectite is detected by the presence of the peak at 14.99 Å of the

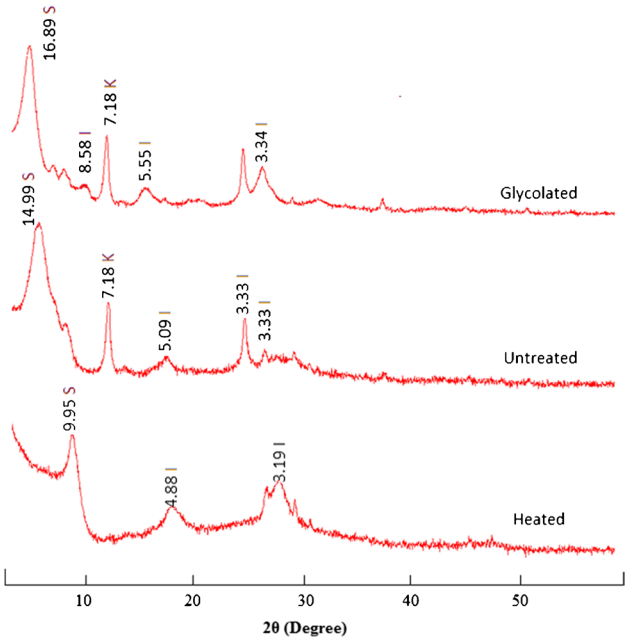

Fig. 3 Natural clay material XRD

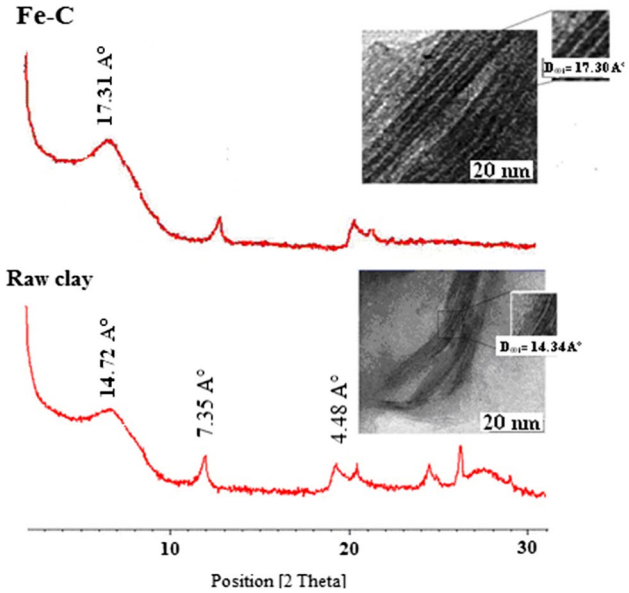

Fig. 4 XRD and MET of raw and modified clay material

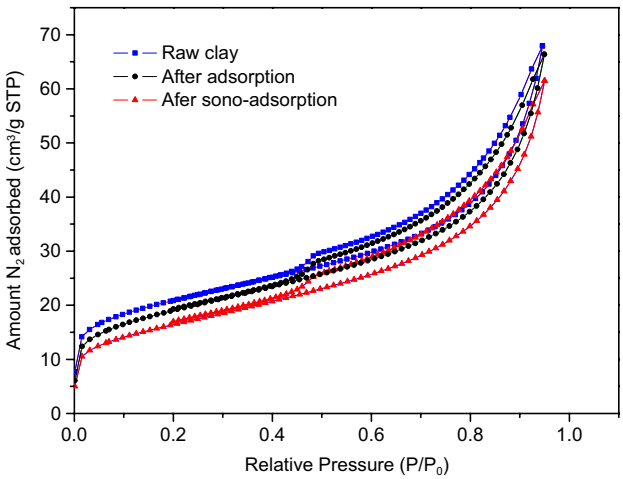

Fig. 5 Nitrogen adsorption–desorption isotherms of samples

unmodified sample which was distended to 16.89 Å on the glycolated sample diffractogram.

The detection of kaolinite is confirmed by the diffraction of the peak at 7.18 Å on the normal and glycolated samples. This peak disappears in the heated sample at 540 °C for 4 h. The reflection instead of peaks at 4.88 and 3.19 Å confirms the existence of illite.

The aforementioned data suggest that this clay is a mixed smectite-illite mineral. After iron-oxide integration, it was noted the d-spacing of smectite was detected at 17.31 Å, and the coupled XRD and TEM images further confirm the intercalation success (Fig. 4).

The nitrogen adsorption/desorption isotherms of the natural Tunisian clay before and after dye adsorption is illustrated in Fig. 5. Nitrogen adsorption for these samples follows a type-IV isotherm which confirmed the presence of mesopores.

Table 1 shows the values of surface area and pore volume intended from the equivalent nitrogen adsorption isotherms characteristic for each material before and after adsorption or sono-adsorption.

The BET surface area of the raw clay before adsorption is 68.32 m^2/g; they became 65.26 and 59.09 m^2/g after adsorption and sono-adsorption, respectively. A decrease in surface area of clay after dye adsorption or sono-adsorption was moreover described in the literature and was credited to the retention within the pores, their padding, and obstruction because of the large dimension of the RB4 molecule (Bel Hadjltaief et al. 2016, Adeogun et al. 2020).

Table 1 Textural properties (N_2 adsorption) of the modified clay before and after treatment

	S_{BET} (m^2/g)	V_P (cm^3/g)	P_D (Å)
Raw clay	68.32	0.190	15
After adsorption	65.26	0.183	21
After sono-adsorption	59.09	0.179	19

Infrared spectra of the used clay before and after RB4 retention are presented in Fig. 6. The IR of used clay noted the presence of O–H vibration which characterizes the presence of hydroxyl groups in the used clay and H_2O molecules

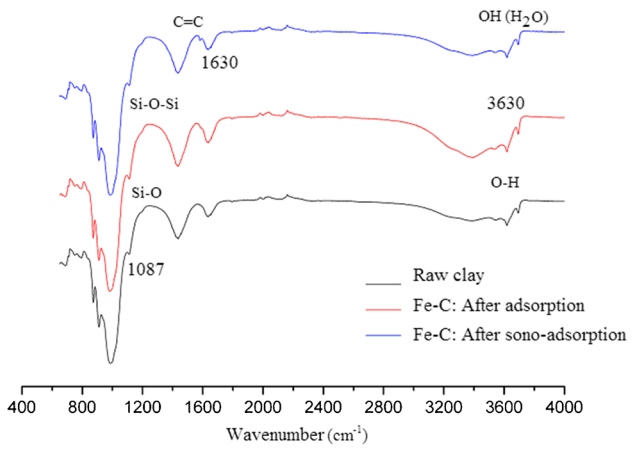

Fig. 6 FT-IR spectra for modified clay material before and after treatment

at 3630 and 3340 cm^{-1}. Further, a vibration of silicates appears between 1200 and 400 cm^{-1}. After modification, a new band vibration was mentioned at 1570 cm^{-1}, which characterizes the presence of aromatic C = C stretching shudders and could evidence the retention of RB4 on the clay. After the dye adsorption, the peak at 1087 was shifted to 1080 cm^{-1}, which can be attributable to interactions of RB4 dye with hydroxyl and Si–O bands.

Effect of pH

Figure 7 presents the impact of pH on the RB4 elimination onto used clay using adsorption and sono-assisted adsorption processes. RB4 removal increases with the raise of the initial pH of the dye solution.

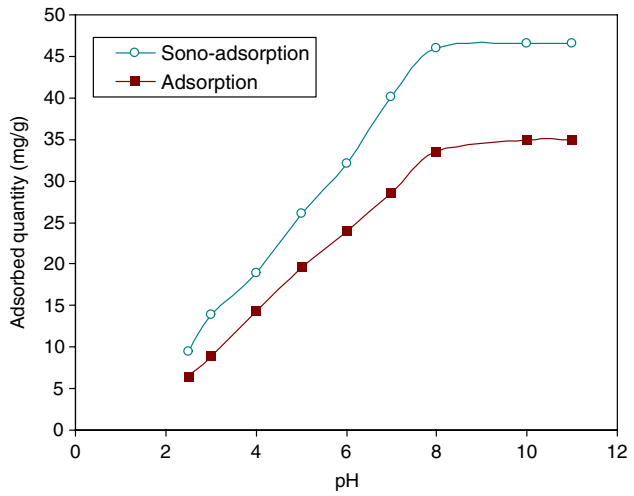

Fig. 7 pH effect on adsorption and sono-assisted adsorption (mass of clay = 0.15 g; concentration of RB4 = 0.2 g/L; time of contact = 20 min; temperature = 25 °C)

For both methods, a maximum of the removal percentage was observed at neutral and basic medium. It was shown that RB4 adsorption is unfavorable at a low pH value (< 4) because of the existence of H^+ ions that fight with the RB4 positively charged for the retention sites (Miyah et al. 2017; Karmakera et al. 2020).

At higher pH (> 7), the surface of used clay will be further negatively charged which triggered the organization between the cationic RB4 dyes and the surface of the adsorbent (Mittal et al. 2010; Sabna et al. 2016). Comparable results have been noted in the literature. Therefore, pH 8 was well-respected as the most favorable value for the RB4 removal.

Effect of adsorbent amount

The adsorbent mass is another interesting parameter as it sets not only the retention amount for the RB4 concentration already determined or fixed but also the system sorbent-sorbate equilibrium. The effect of the adsorbent dose was studied at a variety of adsorbent masses from 0.02 to 0.2 g.

The obtained results are illustrated in Fig. 8. The removal amount of the dye amplified with the adsorbent mass increased from 0.025 to 0.15 g and the most excellent adsorption efficiency of RB4 was obtained with a mass of 0.15 g. The RB4 removal using sono-adsorption reached 46 mg/g within 20 min. The increase in the adsorbent amount leads to an increase in the removal percentage.

This result can be expounded by the availability of adsorption sites on the clay adsorbent (Miyah et al. 2017; Fabryanty et al. 2017). On the other hand, for both processes, the RB4 uptake by clay uttered as retention capacity lessen with the rise in the adsorbent quantity owing to saturation of the adsorption sites resulting to aggregation, resulting in

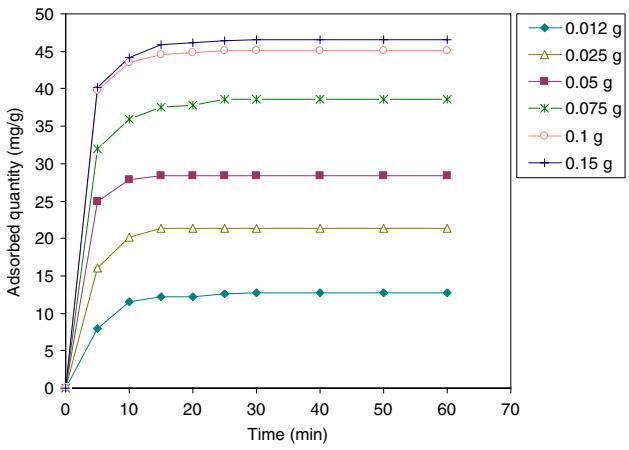

Fig. 8 Adsorbent amount effect on RB4 adsorption and sono-assisted adsorption (pH = 8; concentration of RB4 = 0.2 g/L; time of contact = 20 min; temperature = 25 °C)

an amplification in the diffusion way extent and a decreasing in the total surface area of the clay adsorbent (Sarma et al. 2016). For further studies, an optimum of 0.15 g adsorbent amount should be considered for both processes.

Effect of contact time and dye concentration

The contact time effect on the sono-assisted adsorption of RB4 onto the sample was studied in the concentration range varying from 12.5 to 200 mg/L at pH = 8 and room temperature for a duration of 60 min. In Fig. 9A, the maximum adsorbed amount value of RB4 using sono-assisted adsorption was 33 mg/g in an initial concentration of 50 mg/L. The adsorbed amount rapidly amplified with initial dye concentrations from 12.5 to 50 mg/L.

Nevertheless, when the initial dye concentrations were 100–200 mg/L, sono-assisted adsorption achieved stable states. This might be owing to the concentration of the initial dye. It provides an important conducting force to overcome all of the mass move borders of dye between the aqueous and solid phases. On the other hand, as seen in Fig. 9A, the removal of RB4 was quick in the primary levels of contact time and addressing equilibrium after less than 15 min using sono-assisted adsorption. According to Fig. 9B and during the same time (20 min), it is noticed that the dye was completely degraded using the sono-assisted adsorption. However, in the adsorption process, the dye still persists.

This outcome validates the results obtained from previous works that reported the elimination of various dye molecules of watery solutions per other adsorbents like nanoparticles

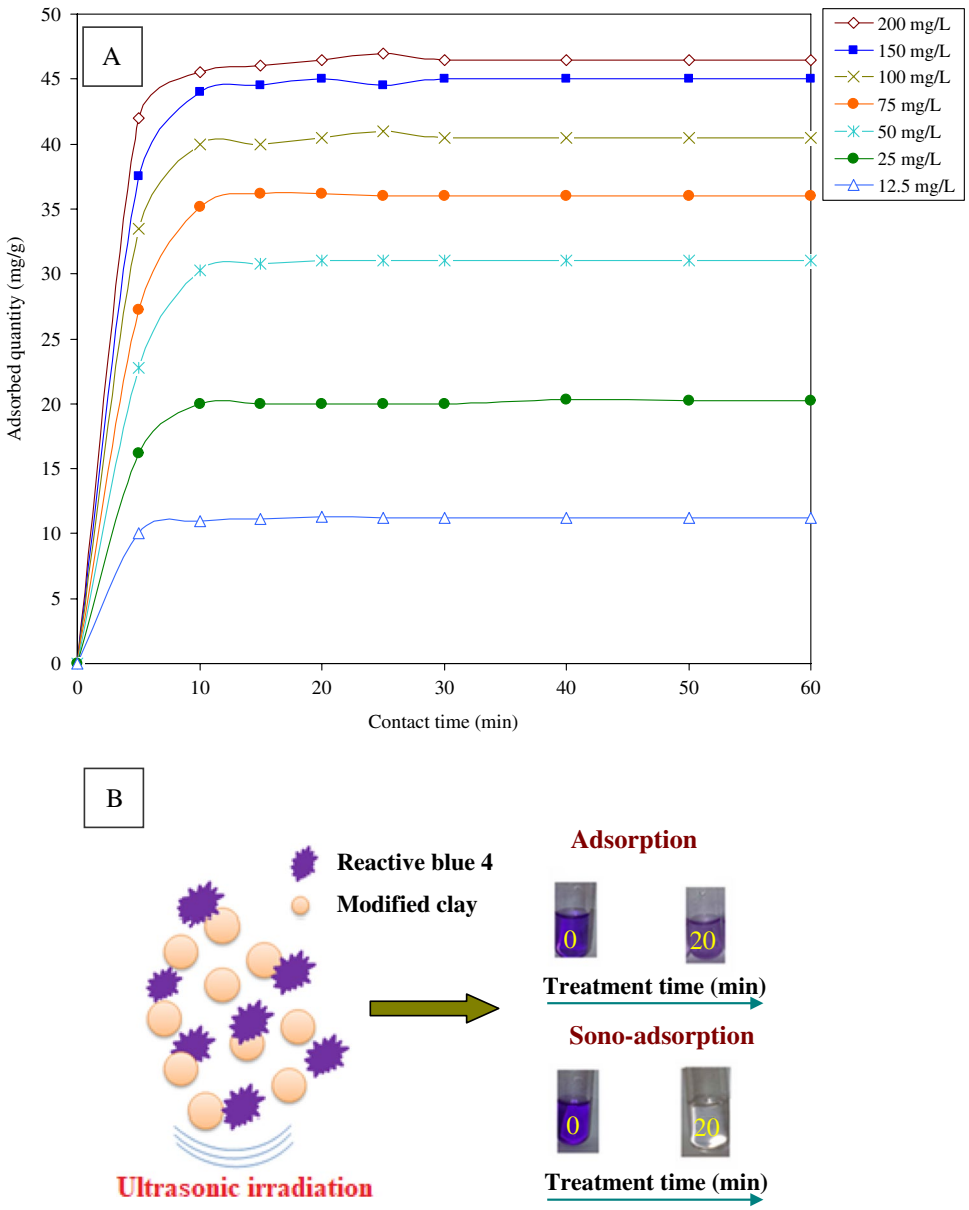

Fig. 9 Contact time and concentration effect on sono-assisted adsorption of RB4 onto modified clay material (A) and efficiency comparison between adsorption and sono-assisted adsorption of RB4 on same time (B) (mass of clay = 0.15 g; pH = 8; temperature = 25 °C)

(Milenković et al. 2013) silica nanopowder (Zhai et al. 2020), and activated carbon (Roosta et al. 2014; Asfaram et al. 2015).

These studies show that ultrasonic radiation improves the surface porosity of the clay, the cavitation's method, and the mass transport amount around the liquid–solid, which increased the diffusion process. These phenomena push dye molecules into the porous structure of the adsorbent, creating more active adsorptive sites, which consequently lead to enhancing the RB4 removal.

Kinetic models

Both pseudo-first- and pseudo-second-order models (Sellaoui et al. 2021) were used to determine the retention process and understand the experimental results of RB4 sono-adsorption by using samples at a variety of concentrations. The Lagergren relation based on the adsorbed quantity presents the pseudo-first-order model. The first speed equation was set to explain adsorption kinetics in an L/S system.

The pseudo-first-order assimilation can be written as follow:

$$ln\left(q_e - q_t\right) = ln\left(q_e\right) - K_1 t \tag{2}$$

where, q_t and q_e (mg/g) are the RB4 doses adsorbed per unit mass at equilibrium and at any time t, respectively. K_1 is the first-order rate coefficient (mn^{-1}). The data of K_1 and q_e intended using the slope and waylay of the linear plot of Ln (q_e-q_t) versus t, respectively.

The following relation represents this model of pseudo-second-order:

$$\frac{t}{q^t} = \frac{1}{K_2 q^2} + \frac{t}{q_e} \tag{3}$$

where, t is time (min), qt is the amount of adsorbate adsorbed per mass of adsorbent at time t (mg g^{-1}), K_2 is the pseudo-second-order rate constant (g mg^{-1} min^{-1}), and q_e is the amount of adsorbate adsorbed at equilibrium (mg g^{-1}).

According to Table 2, the pseudo-second-order confirmed that chemisorption is revealing and controlling the adsorption as rate-limiting step.

Isotherms

In this work, the equilibrium data obtained for the adsorption of RB4 on the modified clay was analyzed by using the isotherm models of Langmuir and Freundlich. Those last, usually specified the aqueous adsorption. Langmuir's model supposes that adsorption takes place at specific homogeneous sites on the surface of the modified clay. Therefore, Freundlich's model qualified for the heterogeneous surface with different energy of material. The Langmuir and Freundlich isotherms can be expressed by the following equations (Eq. (4) and Eq. (5):

$$q_e = \frac{Q_{max} K_L C_e}{1 + K_L C_e} \tag{4}$$

$$q_e = K_F \left(C_e\right)^{1/n} \tag{5}$$

where, q_e (mg/g) is the amount of crystal violet adsorbed onto the clay at equilibrium, C_e (mg/L) is the equilibrium solution concentration. K_L (L/mg) and K_F are the Langmuir

Table 2 Pseudo-first-order and Pseudo-second-order variables of the RB4 dye adsorption onto modified clay

	Pseudo first order			Pseudo second order		
C_0 (mg/L)	k_1 (mn^{-1})	q_e(mg/g)	R^2	k_2 (g/mg.mn)	q_e(mg/g)	R^2
	Sono-adsorption					
12.5	0.319	07.874	0.9539	0.333	11.274	0.9999
25	0.142	04.969	0.6388	0.079	20.492	0.9997
50	0.352	34.182	0.9825	0.043	31.546	0.9993
75	0.381	42.453	0.9780	0.046	36.496	0.9993
100	0.316	31.143	0.9000	0.060	40.984	0.9997
150	0.167	16.905	0.7523	0.043	45.455	0.9998
200	0.302	30.812	0.9442	0.083	46.729	0.9999
	Adsorption					
12.5	0.256	6.104	0.9510	0.167	6.254	0.9990
25	0.154	10.536	0.9270	0.030	13.908	0.9984
50	0.175	27.056	0.9698	0.011	24.510	0.9947
75	0.175	28.801	0.9813	0.014	29.240	0.9981
100	0.267	35.051	0.9765	0.026	31.348	0.9987
150	0.202	32.140	0.9888	0.020	36.101	0.9993
200	0.203	28.132	0.9842	0.028	36.364	0.9995

and Freundlich constants and Q_{max} (mg/g) is the theoretical maximum adsorption quantity.

Figure 10 shows both adsorption isotherms of RB4 onto modified Tunisian clay at 293 K and pH 8, which reveals the relationship between the amount of adsorbed RB4 per unit mass of modified clay (q_e) and the equilibrium concentration in solution (C_e). The parameters for each model were fitted by non-linear regression and are listed in Table 3.

The sono-adsorption equilibrium obtained from the Langmuir possesses a high regression coefficient higher than the Freundlich isotherm. Consequently, the Langmuir isotherm was suitable to describe the sono-adsorption process. The highest adsorption efficiency of RB4 was 48.39 mg/g and 58.52 mg/g using adsorption and sono-assisted adsorption. The RB4 amount adsorbed on the iron-clay in sono-assisted adsorption was greater than that of the adsorption process. This result confirmed those found by Milenković et al. (2013) who studied the removal of 4-dodecylbenzene sulfonate (DBS) from aqueous solutions by corn cob–activated carbon. The results show that the maximum adsorption capacities of the adsorbent, calculated from the Langmuir isotherms, were 29.41 mg/g and 27.78 mg/g in the presence of DBS and its absence, respectively. Enhanced adsorption capacities were ascribed to the presence of the cavitations which ameliorates the ability of the porous clay structure for RB4 retention and the manifestation of novel sites of retention, by disturbance of sorbent particles.

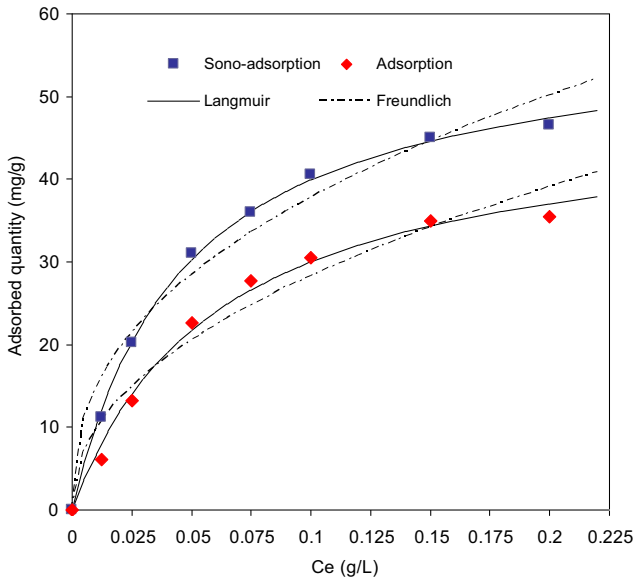

Fig. 10 Modeling of experimental isotherm data of adsorption and sono-adsorption

Comparison of RB4 adsorption efficiency with other adsorbents

In this work, the RB4 removal on iron-modified clay was evaluated with other studies. The obtained maximum quantity (46.51 mg/g) was compared with the data (29.85 mg/g) given by Younes et al. 2021, where the adsorption of reactive yellow 160 dye from textile wastewater was studied using natural and modified glauconite. Similar result was detected in the study of Belachew and Bekele, 2019, which synthesized iron-intercalated bentonite for enhanced adsorption of congo red dye. Moreover, no significant difference was noticed in the obtained result (59.88 mg/g) in the work of Oukebdane et al. 2022 which reports on the adsorption of anionic and cationic Azo-dyes on Fe_3O_4-bentonite magnetic nanocomposite.

Regeneration of Fe–C

The stability of clay adsorbent was tested in five consecutive experiments by two methods, i.e., classic regeneration with N_2 flow and cleaning under O_2/UV. Hamza et al. 2020 detailed the experimental protocol of both methods. Between each experiment, the sample was removed, washed, and fired, at 60°Cfor 12 h. As seen in Table 4, the removal of dye amount using the Fe–C decreases slowly with the rise of recycling number. The dye removal amount of the third cycle was 95% using classic regeneration, whereas treatment efficiency with O_2/UV attends only 86%. The results indicate that cyclic use of modified clay has good stability.

Table 4 Regeneration effect on RB4 sono-adsorption onto modified clay

	1 run	2 run	3 run	4 run
Cleaning under O_2/UV (%)	100	92.13	86.21	73.80
Classic regeneration (%)	100	100	95.11	90.40

Table 3 Langmuir and Freundlich isotherm parameters of RB4 adsorption

	Langmuir			Freundlich		
	Q (mg/g)	K_L (L/g)	R^2	K_F	n	R^2
Adsorption	48.393	16.301	0.996	82.698	2.144	0.978
Sono-adsorption	58.523	21.394	0.999	97.186	2.432	0.985

Conclusions

This study confirmed that the sono-vibration method is a useful method in increasing the mass transport process and set that the used material is a preferment adsorbent on the ability to remove RB4 dye with a high retention capacity. The effects of various parameters such as contact time and temperature on the removal of the dye by adsorption and sono-adsorption were investigated. RB4 removal increased with pH increase up to 10. As well, the concentration increased for both adsorption and sono-adsorption experiments, hence an increase in the number of available adsorption sites. The RB4 removal kinetic by modified clay showed an equilibration time of less than 15 min for sono-adsorption experiments. These results confirmed that the pseudo-second-order kinetic and Langmuir equilibrium model adequately described the RB4 retention onto modified clay with a maximum adsorption capacity of 46.51 mg/g. It was concluded that ultrasonic adsorption was faster than the adsorption process. Consequently, it can be effectively used as an adsorbent for the RB4 adsorption from wastewaters.

Acknowledgements The authors thank Mr Nidhal Baccar, Laboratory technician (Center of Biotechnology of Sfax) for analyzing FTIR samples. They would also like to express their thanks to Dr. Abdelmajid Dammak (Professor at the University of Sfax) for the English revision of this work.

Declarations

Conflict of interest The authors declare that they have no competing interests.

References

Adeogun A, Osideko OA, Idowu M, Shappur V, Akinloye O, Babu BR (2020) Chitosan supported CoFe2O4 for the removal of anthraquinone dyes: kinetics, equilibrium and thermodynamics studies. SN Appl Sci 2. https://doi.org/10.1007/s42452-020-2552-3

Ali F, Reinert L, Levêque J-M, Levêque JM, Duclaux L, Muller F, Saeed S, Shah SS (2014) Effect of sonication conditions: solvent, time, temperature and reactor type on the preparation of micron sized vermiculite particles. Ultrason Sonochem 21:1002–1009

Almazán-Sánchez PT, Linares-Hernández I, Marcos J, Solache-Ríos M-M (2016) Textile wastewater treatment using iron-modified clay and copper-modified carbon in batch and column systems. Water Air Soil Pollut 227:100. https://doi.org/10.1007/s11270-016-2801-7

Amami-Hamdi A, Dhahri F, Jomaa-Salmouna D, Ben Ismail-Lattrache K, Ben Chaabane N (2016) Quantative analysis and paleoecology of Middle to Upper Eocene Ostracods from Jebel Jebil, central Tunisia. Rev Micropaléontologie 59:409–424

Asfaram A, Ghaedi M, Hajati S, Goudarzi A, Bazrafshan AA (2015) Simultaneous ultrasound-assisted ternary adsorption of dyes onto copper-doped zinc sulfide nanoparticles loaded on activated carbon: Optimization by response surface methodology. Spectrochim Acta Part A Mol Biomol Spectrosc 145:203–212

Becelic-Tomin M, Dalmacija B, Rajic L, Tomasevic D, Kerkez D, Watson M, Prica M (2014) Degradation of anthraquinone Dye Reactive Blue 4 in pyrite ash catalyzed Fenton reaction. Sci World J. https://doi.org/10.1155/2014/234654

Bel Hadjltaief H, Ben Zina M, Galvez ME, Da Costa P (2016) Photocatalytic degradation of methyl green dye in aqueous solution over natural clay-supported ZnO–TiO_2 catalysts. J Photochem Photobiol A Chem 315:25–33

Belachew N, Bekele G (2019) Synergy of magnetite intercalated bentonite for enhanced adsorption of congo red dye. SILICON 12:603–612. https://doi.org/10.1007/s12633-019-00152-2

Ben Ameur S, Barhoumi A, Bel hadjltaief H, Mimouni R, Duponchel B, Leroy G, Amlouk M, Guermazi H (2017) Physical investigations on undoped and Fluorine doped SnO2 nanofilms on flexible substrate along with wettability and photocatalytic activity tests. Mater Sci Semicond Process 61:17–26

Bethi B, Manasa V, Srinija K, Sonawane SH (2018) Intensification of Rhodamine-B dye removal using hydrodynamic cavitation coupled with hydrogel adsorption. Chem Eng Process - Process Intensif 134:51–57

Chatel G, Novikova L, Petit S (2016) How efficiently combine sonochemistry and clay science. Appl Clay Sci 119:193–201

Chu KH, Al-Hamadani YAJ, Park CM, Lee G, Jang M, Am J, Her NG, Son A, Yoon Y (2017) Ultrasonic treatment of endocrine disrupting compounds, pharmaceuticals, and personal care products in water: a review. Chem Eng J 327:629–647

Dietel J, Warr LN, Bertmer M, Steudel A, Grathoff G, Emmerich K (2017) The importance of specific surface area in the geopolymerization of heated illitic clay. Appl Clay Sci 139:99–107. https://doi.org/10.1016/J.CLAY.2017.01.001

Dil AA, Vafaei A, Ghaedi AM, Ghaedi M, Dil EA (2018) Multi-responses optimization of simultaneous adsorption of methylene blue and malachite green dyes in binary aqueous system onto Ni:FeO(OH)-NWs-AC using experimental design: derivative spectrophotometry method. Appl Organomet Chem 32:4149

Eloussaief M, Bel Hadjltaief H, Dammak N, Benzina M (2018) Valorisation of green algae from Tunisian littoral on dye elimination. Arab J Geosci 11:730

Eloussaief M, Chakroun S, Kallel N, Benzina M (2020a) Efficiency of clay materials collected from Ain Jaloula (Central Tunisia) in sunflower oil decolorization. EuroMediterr J Environ Integr 5:33

Eloussaief M, Hamza W, Ghorbali G, Kallel N, Benzina M (2020b) Fe-rich aragonite concretion applied to industrial dye purification using Fenton and photo-Fenton technologies. Waste Biomass Valorization 12:3303–3313

Eren Z (2012) Ultrasound as a basic and auxiliary process for dye remediation: a review. J Environ Manage 104:127–141

Fabryanty R, Valencia C, Soetaredjo FE, Putro JN, Santoso SP, Kurniawan A, Ju Y-H, Ismadji S (2017) Removal of crystal violet dye by adsorption using bentonite-alginate composite. J Environ Chem Eng 5:5677–5687

Hamza W, Chtara C, Benzina M (2016) Purification of industrial phosphoric acid (54%) using Fe-pillared bentonite. Environ Sci Pollut Res 23:15820–15831

Hamza W, Fakhfakh N, Dammak N, Bel Hadjltaeif H, Benzina M (2020) Sono-assisted adsorption of organic compounds contained in industrial solution on iron nanoparticles supported on clay: optimization using central composite design. Ultrason Sonochemistr 67:105–134. https://doi.org/10.1016/j.ultsonch.2020.105134

Jarraya I, Fourmentin S, Benzina M, Bouaziz S (2016) VOC adsorption on raw and modified clay materials. Chem Geol 275:1–8

Jorfi S, Darvishi Cheshmeh Soltani R, Ahmadi M, Khataee A, Safari M (2017) Sono-assisted adsorption of a textile dye on milk

vetch-derived charcoal supported by silica nanopowder. J Environ Manage 187:111–121

Karmakera S, Naga AJ, Sahaa TK (2020) Adsorption of Reactive Blue 4 Dye onto Chitosan 10B in aqueous solution: kinetic modeling and isotherm analysis. Russ J Phys Chem A 94:2349–2359. https://doi.org/10.1134/S0036024420110126

Kashif Uddin M (2016) A review on the adsorption of heavy metals by clay minerals, with special focus on the past decade. Chem Eng J 308:438–462. https://doi.org/10.1016/j.cej.2016.09.029

Khoualdia B, Loungou M, Elaloui E (2017) Adsorption of organic matter from industrial phosphoric acid (H3PO4) onto activated bentonite. Arab J Chem 10:1073-S1080

Machado AT, Valenzuela-Diaz FR, de Souza CAC, de Andrade Lima LRP (2011) Structural ceramics made with clay and steel dust pollutants. Appl Clay Sci 51:503–506

Milenković DD, Bojić AL, Veljković VB (2013) Ultrasound-assisted adsorption of 4-dodecylbenzene sulfonate from aqueous solutions by corn cob activated carbon. Ultrason Sonochem 20:955–962

Mittal A, Mittal J, Malviya A (2010) Adsorption of hazardous dye crystal violet from wastewater by waste materials. J Colloid Interface Sci 343:463–473

Miyah Y, Lahrichi A, Idrissi M, Boujraf S, Taoudad H, Zerrouq F (2017) Assessment of adsorption kinetics for removal potential of Crystal Violet dye from aqueous solutions using Moroccan pyrophyllite. J Assoc Arab Univ Basic Appl Sci 23:20–28

Oukebdane K, Lacene Necer I, Didi MA (2022) Binary comparative study adsorption of anionic and cationic Azo-dyes on Fe_3O_4-bentonite magnetic nanocomposite: kinetics, equilibrium, mechanism and thermodynamic study. SILICON. https://doi.org/10.1007/s12633-022-01710-x

Roosta M, Ghaedi M, Shokri N, Daneshfar A, Sahraei R, Asghari A (2014) Optimization of the combined ultrasonic assisted/adsorption method for the removal of malachite green by gold nanoparticles loaded on activated carbon: experimental design. Spectrochim Acta Part A Mol Biomol Spectrosc 118:55–65

Sabna V, Thampi SG, Chandrakaran S (2016) Adsorption of crystal violet onto functionalised multi-walled carbon nanotubes: equilibrium and kinetic studies. Ecotoxicol Environ Saf 134:390–397

Sajjadi S, Khataee A, Kamali M (2017) Sonocatalytic degradation of methylene blue by a novel graphene quantum dots anchored CdSe nanocatalyst. Ultrason Sonochem 39:676–685

Sarma GK, Sen Gupta S, Bhattacharyya KG (2016) Adsorption of Crystal violet on raw and acid-treated montmorillonite, K10, in aqueous suspension. J Environ Manage 171:1–10

Sellaoui L, Dhaouadi F, Reynel-Avila HE, Mendoza-Castillo DI, Bonilla-Petriciolet A, Trejo-Valencia R, Taamalli S, Louis F, El Bakali A, Chen Z (2021) Physicochemical assessment of anionic dye adsorption on bone char using a multilayer statistical physics model. Environ Sci Pollut Res. https://doi.org/10.1007/s11356-021-15264-9

Soltani RDC, Jorfi S, Safari M, Rajaei M-S (2016) Enhanced sonocatalysis of textile wastewater using bentonite-supported ZnO nanoparticles: response surface methodological approach. J Environ Manage 179:47–57

Ullhyan A (2014) Adsorption of reactive blue-4 dye from aqueous solution onto acid activated mustard stalk: equilibrium and kinetic studies. Glob J Biol Agric Health Sci 3:98–105

Wu TY, Guo N, Teh CY, Hay JXW (2013) Theory and fundamentals of ultrasound. In: Advances in utrasound technology for environmental remediation. Springer Briefs in Molecular Science, Green Chemistry for Sustainability. https://doi.org/10.1007/978-94-007-5533-8

Younes H, El Etriby H, Kh MH (2021) High removal efficiency of reactive yellow 160 dye from textile wastewater using natural and modified glauconite. Int J Environ Sci Technol. https://doi.org/10.1007/s13762-021-03528-3

Zhai Y, Qu H, Li Z, Zhang B, Cheng J, Zhang J (2020) Rapid and efficient adsorption removal of Reactive Blue 4 from aqueous solution by cross-linked microcrystalline cellulose-epichlorohydrin polymers: isothermal, kinetic, and thermodynamic study. Transactions of Tianjin University 27:77–86. https://doi.org/10.1007/s12209-020-00245-9